Biological effects of polystyrene micro- and nano- plastics on human intestinal organoid-derived epithelial tissue models without and with M cells

Ying Chen[1*], Ashleigh M. Williams[1], Edward B. Gordon[1], Sara E. Rudolph[1], Brooke N. Longo[1], Gang Li[1,2], David L. Kaplan[1*]

[1] Department of Biomedical Engineering
Tufts University
4 Colby St
Medford, MA, 02155
USA

[2] National Engineering Laboratory for Modern Silk
College of Textile and Clothing Engineering
Soochow University
Suzhou 215123, China

*To whom correspondence may be addressed. Email: ying.chen@tufts.edu; david.kaplan@tufts.edu.

Abstract

Plastic pollution has been recognized as a severe and growing environmental issue. Micro- and nano-plastics (MPs and NPs) released from these plastics in the environment can enter the food chain and target the human intestine. However, knowledge about the effects of MPs and NPs on the human intestine is still limited due to the lack of human clinical studies or a relevant human intestine tissue model to validate data obtained from animal studies or cell and tissue models that employ human cancer cells. In this study, human tissue organoids were used to develop human intestinal epithelia to mimic the cell complexity and biological functions of native tissue. Further, the expression of Microfold cells (M cells) was induced in the differentiated monolayers to distinguish their role to exposure of MPs and NPs. Polystyrene (PS), the predominant commercial plastic, was chosen for the study. We investigated and compared the impact of PS particles in the intestinal monolayers with and without M cells with varying sizes (1 μm, 500 nm, 100 nm, and 30 nm), concentrations (250, 500, and 1000 μg/mL), and exposure periods (24, 48, 72 and 96 hours). During the exposure, the M cells fulfilled their role as sensers, capturers and transporters of larger sized PS particles. We determined that the human intestinal epithelial cells internalize PS particles in a size-, concentration-, and time-dependent manner. Importantly, high concentrations of particles significantly triggered the secretion of inflammatory cytokines, TNF-α, TGF-β1, IL-6 and IL-8, linked to human inflammatory bowel disease (IBD), suggesting a link between the ingestion of PS MP and NP and IBD. The present study demonstrated the utility of human intestinal organoids in assessments of impact of PS ingestion on intestinal physiology and the results provide insights into plastic particle management and control if needed.

1. Introduction

Plastics are some of the most ubiquitous manmade materials and they have pervaded nearly every aspect of human life. It is estimated that 8.3 billion metric tons of virgin plastic has been generated as of 2017, and this number is expected to more than double by 2050.[1] Plastic waste comprises around 10% of municipal waste by mass and has become one of the most pressing environmental issues due to the non-biodegradable nature of most plastics, combined with visible accumulation in freshwater, wastewater, marine waters, on beaches and in many animals.[2] This accumulation is, in part, due to the fact that most plastics can break down into very small particles. Particles between 1 and 1,000 μm in diameter are considered microplastics (MPs); while plastic particles between 1 and 100 nm (or up to 500nm in some instances) are known as nanoplastics (NPs).[3] MPs/NPs have been consistently detected in seafood, various convenience foods and beverages, and in tap/bottle water.[4] MPs/NPs are also distributed in and accumulate within living organisms in different tissues, including the digestive tract, blood, liver, pancreas, heart and, notably, the brain.[5] In 2018, microplastics were first reported in human feces, providing evidence of accumulation, ingestion and excretion of these particles in humans and indicating exposure through processed or packaged food/water consumption.[6] The mass of MPs and NPs ingested by the human body ranges from 0.1-5 g/person/week based on an average mass of an individual plastic particle derived from different studies and oral intake from sources such as shellfish, salt, beer and drinking water.[7] As human exposure to MPs and NPs continues to grow, MPs and NPs have been recognized as emerging contaminants within the last decade. These particles raise concerns for human and environmental health due to their environmental persistence, potential (eco)toxicity, ability to accumulate in different tissues, and ability to act as carriers or vectors of toxic chemicals upon ingestion, including pathogens.[4]

Investigations of the impact of MPs/NPs on organism health after oral uptake have been widely conducted in mammalian (rodent) models and ingestion has been demonstrated as the main pathway for the uptake of MPs/NPs.[8] Ingested MPs/NPs first encounter the intestinal epithelium, the innermost layer of the mucosa, where most digestive, absorptive and secretory processes occur. This makes the intestine the primary exposure site for these particles and particularly important in terms of assessments of the impact of plastics on physiological functions. In mice, ingested MPs and NPs accumulated in the gut, including those composed of the most common polymers, polystyrene (PS), polyethylene (PE), and polypropylene (PP). PS accumulated as both NPs (25-500 nm) and MPs (0.5-50μm) while PE accumulated between the NP and MP range (500 nm-1μm).[9-12] Pathological changes to the gut included a reduction in the production of intestinal mucus, intestinal epithelial barrier dysfunction (e.g., decreased Zonula occludens-1 (zo-1) and Claudin 1), intestinal inflammation with upregulation of proinflammatory cytokines and dysbiosis of the gut microbiota.[9] Pregnant mice exposed to PS MPs during gestation and lactation have a higher risk of metabolic disorders in their offspring.[13] In addition, accumulation of MPs in mouse in liver, kidney and gut was detected after 28 days (@0.5 mg/day) and this accumulation led to significant alterations in several biomarkers that indicated potential toxicity from this longer-term exposure.[9] In all cases, the effects in the gut correlated with size and morphology of the plastic particles, exposure concentration, exposure time, and tissue uptake and accumulation. However, there have also been studies that failed to demonstrate that MPs/NPs had a significant effect on animals. For example, a rat model showed a very low number of MPs taken up by intestinal tissue and the authors did not detect any histological lesions or significant inflammatory responses in the gut of the animals.[14] Another study using rats to analyze potential neurobehavioral effects of PS NPs did not identify statistically significant behavioral changes or abnormalities.[15] These results represent an important clue to the accumulation and release of MPs/NPs following exposure to mammals, with remaining controversy regarding biological impact. In part, the variable outcomes above reflect the lack of studies specifically focused on human intestinal outcomes, which would presumably help to clarify the impact.

Despite the many studies on animals, toxicological evaluations of MPs/NPs on the human intestine in vivo are still lacking. As mentioned above, the intestine is considered the major route for particle exposure.

The makeup of the native intestinal epithelium is diverse and populated with multiple differentiated epithelial cells, including enterocytes (absorption), goblet cells (mucus secretion), enteroendocrine cells (peptide and hormone production) (EECs), Paneth cells (antimicrobial protein secretion), and microfold cells (M cells, immune sensing and uptake of particulate microbial antigen).[16] In addition to its primary function of nutrient digestion and absorption, the intestinal epithelium also provides a protective barrier via apical intercellular junctions which protect against physical, chemical, and biological damages.[17] Thus far, studies exploring the interactions between MPs/NPs and human intestinal cells have been mainly performed with monocultures of human colorectal adenocarcinoma epithelial cell-lines, Caco-2 (enterocyte-like cells) or HT29-MTX (goblet-like cells).[18, 19] To achieve slightly more physiological conditions, many researchers have employed a Caco-2/HT29-MTX coculture system as an in vitro experimental model.[20] To further improve upon this system, some researchers also include lymphoblast-like Raji-B cells to induce Caco-2 cells into microfold-like cells.[21] Most of these studies, while revealing some level of cellular uptake and epithelial transport of MPs/NPs, showed either low or insignificant cytotoxic effects, except at very high concentrations of particles. Overall, these prior studies have not identified severe acute cytotoxic effects but have demonstrated the potential for low to moderate damage of the cells and tissues depending on the size and concentration of MPs/NPs. The degree of cellular uptake of the particles was somewhat consistent with the observations in animals. For example, 44 nm PS NPs strongly upregulated cytokine levels of IL-1β, IL-6, and IL-8 compared to 100 nm PS NPs in human gastric adenocarcinoma epithelial cells.[22] PS particles (sizes 200 nm-30μm) did not show significant toxicological impact on human cells at concentrations up to 500 μg/mL [23]. Of note, these in vitro findings were all from short-term studies (up to 48 hours of exposure) with MPs/NPs exposed to human intestinal epithelial cell lines, whereas it can take up to 14 days for microplastics to pass through marine animals (compared to a normal digestion period of 2 days).[24] Moreover, the intestinal epithelial cell cultures used for cytotoxicity studies were based on cancerous cell lines and were missing other important intestinal epithelial cell types. Consequently, these studies do not fully capture the cellular complexity of the native human intestine, thus, fall short of biological processes in vivo. Therefore, knowledge gaps still exist on the mechanisms and predictions regarding acute and chronic effects caused by these plastics in humans.

Thanks to advances in stem cell biology, organoids have been established as new model system for biomedical research and have been extensively reviewed.[25] Organoids are in vitro miniaturized organ models originating from self-organizing stem cells. Compared to conventional cancerous cell lines, organoids are capable of physiologically mimicking the in vivo structure and function of an organ. They can be produced from adult (murine and human) stem cell-containing tissue samples, organ-specific single adult stem cells (ASCs), embryonic stem cells (ESCs), or induced pluripotent stem cells (iPSCs) and expanded indefinitely with the support of a cocktail of various growth factors in their culture media. Organoids can be grown to model many human organs, including the stomach, intestine, kidneys, heart, pancreas, brain, and liver. For the human intestine, organoids can be generated from fresh or frozen patient biopsies of intestinal tissue specimens by isolating crypts, the intestinal stem cell niche.[26] The isolation procedure yields spheroid-shaped and budding organoids which become ever-expanding in a 3D Matrigel in the presence of Wingless-related integration site (Wnt) pathway agonist, R-spondin (Rspo), epidermal growth factor (EGF), and the BMP inhibitor, Noggin.[27] As these organoids contain stem cells, they have the ability to differentiate toward different intestinal epithelial cell lineages. For specific (and rare) cell types, the differentiation protocols for intestinal organoids have been updated and standardized to direct stem cell maintenance or differentiation toward specific cell fates. For example, by removing the Wnt, Noggin, and R-spondin from the culture media, the organoids simultaneously differentiate into a continuous intestinal epithelium containing enterocytes, goblet cells, EECs, and Paneth cells with an abundance that is similar to what is found in vivo.[28, 29] By treating the organoids with nucleic factor-kappa B ligand (RANKL), a common M cell inducer, increased M-cell differentiation can be achieved in the cultures.[30] Over the past decade, intestinal organoids have been derived from healthy and diseased intestinal tissues and can be used as an alternative to Caco-2 drug absorption and permeability assays for drug screening and

for personalized medical decisions to better predict patients' treatment response and, importantly, any potential drug toxicity.[31]

We have previously used human intestinal organoids from both large and small intestine for intestinal tissue engineering,[32] inflammatory bowel disease modeling,[33] and host cell-microorganism interactions.[28] In the present study, we explored the application of these organoids as a platform for predicting potential risks of MP and NP exposure. Specifically, the goals of this work were: 1) to establish and characterize two organoid-derived intestinal epithelial monolayer models: monolayers without M cells (enterocytes, goblet cells, EECs, and Paneth cells) and monolayers with M cells (enterocytes, goblet cells, EECs, Paneth cells, and M cells); 2) to compare the dynamics of cellular uptake and translocation of different sizes of MPs and NPs over time in these two different tissue models; 3) to evaluate the potential dose-, size- and exposure period-dependent cytotoxic effects of the plastic particles on the intestinal barrier integrity and immune response in the tissue models; 4) to distinguish the role of M cells regarding the transport of plastic particles across the intestinal epithelium and how M cells shape specific immune responses to these particles. In this work, PS MPs and NPs were selected as the model particles for the following reasons: 1) they are commercially available with a wide range of specific sizes; 2) they are fluorescently labeled, allowing for localization and tracking in cell compartments; and 3) they are biologically stable in various cell culture media.

2. Materials and methods (included in Supplementary Materials)

3. Results

3.1 Characterization of PS MPs and NPs

PS MPs and NPs in different sizes (1 μm, 500 nm, 100 nm, and 30 nm) and fluorescently labeled are commercially available from Sigma Millipore. All the plastic particles diluted in DMEM were detected using fluorescence microscopy and SEM to validate the manufacturing sizes and the fluorescence. Microscopy images showed significant fluorescence signals from different sizes of particles confirming the fluorescence labels on the particles (Figure 1). In addition, a uniform dispersion of particles without significant aggregation was detected in DMEM (Figures 1A-D). SEM images further confirmed that all particles (Figures 1E-H) had a spherical shape. To statistically evaluate particle size, Image J and SPSS were used to analyze the means, standard deviations, and ranges of particle sizes in the SEM images (Table 1). Mean particle sizes were equivalent to labeled specificities (Table 1, Column 3). The particle sizes ranged from 28.56 to 31.82 nm for 30 nm NPs, from 97.13 to 104.25 nm for 100 nm, from 494.92 to 503.89 nm for 500 nm, and from 0.870 to 1.25 μm for the 1 μm MPs, respectively (Table 1, Column 5).

3.2 Establishment and characterization of human intestinal organoid derived monolayers with and without induced M cells

Human intestinal organoids (Figure 2A-B) derived from ileum biopsy specimens were subcultured for monolayer generation. For monolayer preparation, organoids were enzymatically dissociated into single cells and seeded onto transwell inserts. Monolayers reached confluence 1-2 days post seeding (Figure 2C). After that, the monolayers were either treated with Standard Differentiation Medium (SDM) or M-cell Differentiation Medium (MDM) to establish intestinal epithelia both with and without M cells (Figure 2A). SDM and MDM have been widely utilized to generate well-differentiated epithelia derived from intestinal organoids.[30, 32, 34] Organoid-derived epithelial monolayers treated with SDM for 3 days simultaneously differentiated into enterocytes, goblet cells, Paneth cells, enteroendocrine cells, while monolayers supplemented with MDM basolaterally for 6 days differentiated into enterocytes, goblet cells, Paneth cells, enteroendocrine cells, and M cells.

To confirm that these different major cell types were present in the differentiated monolayers, we collected and stained the SDM-differentiated monolayers at day 3 and day 6 post-differentiation to confirm the presence of relevant marker proteins (Figure 2D-I). As expected, SDM-differentiated cell cultures expressed sucrase-isomaltase (SI, Figure 2D) signal in the apical region of enterocytes throughout the

monolayers, the mucin 2 (MUC2, Figure 2E) staining in a scattering of goblet cells, the Lysozyme expression (Figure 2F) by Paneth cells, and the induction chromogranin A (ChgA, Figure 2G) positive EECs. Furthermore, immunostaining also revealed the typical "chicken wire" staining pattern of ZO-1 tight junction protein (Figure 2H and 2I), suggesting the individual mature epithelial cells are joined to their neighbors to assemble the tight junction network in the epithelium for maintenance of epithelial barrier integrity. A similar staining pattern of the above-mentioned markers was observed in MDM-differentiated epithelial monolayers (data not shown). To determine if MDM successfully induced M cells along with the major epithelial cell types in the monolayer cultures, immunofluorescence using M cell specific cell surface marker, glycoprotein 2 (GP2), was performed on MDM-differentiated epithelial monolayers. Immunofluorescence analysis showed that a significant amount of the M cells developed in the monolayers 6 days after treatment with MDM, as shown by the immunostaining for GP2 (Figure 2I and Sup Figure 1A). Moreover, by SEM, the differentiated monolayers displayed an apical-basolateral polarization of epithelial cells indicated by the presence of tightly packed microvilli at the apical side with random distribution of "bald" M cells with disorganized stubby microvilli along their apical border (Figure 2J and 2K). Overall, these observations indicated that organoid-derived epithelial monolayers properly differentiated into the major intestinal epithelial cell types without or with M cells using SDM or MDM.

Differentiation of the organoid-derived monolayers was further evidenced by the significantly increased TEER values after switching to differentiation media in SDM- and MDM-differentiated epithelial monolayers (Figures 2L-M). Fully differentiated SDM-treated cultures possessed a TEER between 627 and 726 $\Omega*cm^2$ (Figure 2L); while full differentiated MDM-treated cultures feature a TEER between 396-495 $\Omega*cm^2$ (Figure 2M). TEER values are strong indicators of epithelial maturation and integrity of the cellular barrier [35]. The fully differentiated MDM-treated monolayers demonstrated a lower TEER value suggesting greater permeability and better represent in vivo intestine permeability (small intestine: 50-100 $\Omega.cm^2$; colon: 300-400 $\Omega*cm^2$) [35] compared to SDM-treated monolayers.

3.3 Cellular binding, uptake and translocation of PS MPs and NPs in human intestinal epithelia

Next, we investigated the potential cytotoxic effects of PS MPs and NPs on human intestinal epithelial cells. Towards this goal, we first explored the interactions between the plastic particles and the gastrointestinal epithelium by studying the cellular binding, uptake and translocation of the particles by the intestinal epithelium. The two different intestinal organoid-derived epithelial models, as established in section 3.2, were employed: the SDM-differentiated monolayers (enterocytes, goblet cells, Paneth cells, EECs) and MDM-differentiated monolayers (enterocytes, goblet cells, Paneth cells, EECs, and M cells). After the cell seeding and differentiation with SDM or MDM (Figure 3A), different sizes of spherical fluorescent PS particles (1 μm, 500 nm, 100 nm, 30 nm) were applied on the apical side of the intestinal epithelia at a concentration of 500 μg/mL to explore particle uptake and transport. Samples from two different culture models were harvested 24, 48, 72, 96 hours post dosing and prepared for confocal microcopy and SEM to detect the binding and trace the location of the MPs and NPs in the monolayer cultures. At 24 hours, all MPs and NPs bound to the intestinal epithelial cell surface and M cells (Figures 3B-E and 3J-M), which is a prerequisite for cellular uptake (Figure 3B-E and 3J-M). Exposure to the plastic particles did not significantly affect tight junction formation demonstrated by ZO-1 expression. After 48 hours, in SDM-differentiated monolayers, particle sizes $\leqslant$ 500 nm were imaged "nestling" or being enveloped by surrounding microvilli which may suggest these particles tend to cross the apical microvilli brush border of the epithelial cells (Fig. 3G-I), whereas in the MDM-differentiated monolayers, it was found that larger sized particles (1μm, 500nm) tended to be more specifically aggregated on and bound to the surface of M cells (Figures 3N and 3Q, and sup Figures 1B-C).

The intracellular uptake and translocation of MPs and NPs in the culture systems were tracked for up to 96 hours by confocal laser scanning microscopy (Figures 4 and 5). The three-dimensional image reconstruction of x-z cross-section from confocal sequential acquisition of the fluorescence signals from different planes enabled particle tracing at varying cellular depths. In the SDM-differentiated monolayers, over the course of 96 hours, the 1μm MP group were mainly observed on the apical side (Figure 4A, yellow

arrows) of the intestinal epithelium, suggesting they did not cross the epithelia barriers. For the 500nm MP group, at 96 hours post dosing, most of the particle fluorescence signals were still detected on the apical surface of the intestinal epithelium with occasional translocation across the epithelium, indicating no obvious particle translocation (Figure 4B, yellow arrows). For the 10 0nm NP group, at 96 hours, particle signals started to appear inside some of the epithelial cells and on the basal side of the epithelium (Figure 4C, yellow arrows), suggesting cellular uptake and penetration of NPs. In the 30 nm NP group, at 96 hours, large numbers of particles were found on the basal side of the epithelium (Figure 4D, yellow arrows), suggesting that after cellular binding, the 30 nm NPs were taken up and translocated from the apical to the basal side of the epithelium. The particle tracking results demonstrated an MP/NP size-dependent uptake and translocation, with the highest total for PS uptake for the smallest NPs (30 nm). In the MDM-differentiated monolayers containing M cells, similar intracellular uptake and translocation patterns of 100 nm and 30 nm NPs were identified in the epithelium through 48 hours (data not shown). However, at 72 hours, obvious translocation of 100 nm and 30 nm NPs to the basal side of the epithelia was observed, followed by the degradation of epithelial tight junctions (ZO-1) (100 nm) and the lifting of monolayers from the transwell inserts (30 nm) at 96 hours post particle exposure (sup Figure 2). Furthermore, 1μm and 500 nm particles preferentially internalized and accumulated in M cells as shown in Figure 5 (yellow arrow), suggesting induced M cells demonstrated functionality with increased uptake of larger sized particles ($\geqslant$ 500 nm). In vivo, M cells are specialized to endocytose and transcytose large particulates. Taken together, these results demonstrated that PS MPs and NPs could directly bind and enter intestinal cells and that the efficiency of cellular uptake and transport was dependent on particle size and exposure period.

3.4 Cytotoxicity effect of PS MPs and NPs in human intestinal epithelia

Knowing that different sizes PS MPs and NPs can interact with and cross the human intestinal epithelia, we next assessed their cytotoxic effects by using different concentrations and exposure periods in the human intestinal epithelia. In this study, the toxicity assessment was conducted using two different assays: TEER- to examine epithelial integrity and ELISA- to measure cytokine secretion (inflammatory responses). For cytokine profiling, the release of proinflammatory cytokines interleukin-6 (IL-6), IL-8, tumor necrosis factor-alpha (TNF-α) and an anti-inflammatory cytokine TGF-β1 were analyzed. The two different intestinal organoid-derived epithelial models (with and without induced M cells) were compared. The cytotoxic response of cells treated with MPs and NPs (1 μm, 500 nm, 100 nm, and 30 nm) for 24, 48, 72 and 96 hours was investigated using particle concentrations ranging from 250-1000 μg/mL (250, 500, 1000 μg/mL).

3.4.1 Barrier integrity and cytokine secretion in particle-exposed epithelia without induced M cells

The TEER values of SDM-differentiated monolayers treated with 250, 500, 1000 μg/mL of 1μm, 500 nm, 100nm particles remained relatively constant and equivalent to the control over the duration of the exposure (Figures 6A-C), suggesting the particles did not substantially and adversely affect the intestinal barrier integrity. For the 30nm group (Figure 6D), cellular integrity was not altered by 250 and 500 μg/mL particles until 48 hours (day 5 in culture) post dosing. At 72 hours, 30nm NPs induced a slight decline in TEER values at 1000 μg/mL.

The levels of cytokines (TNF-α, TGF-β1, IL-6, IL-8) in all exposure groups of MPs and NPs (Figures 6E-H) were determined and no significant increase in cytokine secretions were induced from any of the particle groups at 250 μg/mL compared to the control groups. However, at 500 and 1000 μg/mL, secretion of TNFα, IL-6 and IL-8 was significantly increased in the 100 nm and 30 nm NPs after 96 or 72 hours of exposure (**$p < 0.01$, Figures 6I, K and L). By extrapolation, these results demonstrated that the smaller sizes (100 nm and 30 nm) of the PS NPs at concentrations greater than 500 μg/mL might induce the release of pro-inflammatory cytokines (TNF-α, IL-6 and IL-8) in the human intestinal epithelial cells.

3.4.2 Barrier integrity and cytokine secretion in particle-exposed epithelia with M cells

According to the TEER analysis, the epithelial integrity of MDM-differentiated monolayers was not significantly impacted by 1μm and 500 nm particles at any concentration (Figures 7A-B) but was impacted by 100 nm and 30 nm PS particles at 250 and 500 μg/mL over time (Figures 7C-D). However, compared to the control group, a significant decrease (*p<0.05) in TEER value was observed in monolayers that were exposed to 100 nm and 30 nm NP groups at 1000 μg/mL for 48 hours (Figures 7C-D), indicating impaired epithelial barrier function was caused by the exposure to 1000 μg/mL 100 nm and 30 nm particles.

For cytokine production, compared to the control groups, no statistically significant changes were detected for all particle sizes in 250 μg/mL group throughout the exposure course. Increased release of cytokines (TNF-α, IL-6, IL-8) in the 500 ug/mL group were detected and sustained in the 100 nm and 30 nm NPs across various time points (Figures 7I, K, and L) with no obvious changes in TGFβ1 (Figure 7J). Specifically, 500 μg/mL 100 nm NPs triggered a higher release of IL-6 at 72 hours post exposure (Figure 7K) and IL-8 at 48 hours (Figure 7L). Comparatively, the 30 nm NPs significantly triggered TNF-α secretion at 96 hours post exposure and IL-6 and IL-8 secretions as early as 48 hours (Figures 7K-L). In the 1000 μg/mL groups, acute releases of TNF-α and IL-6 by cells were found in all different sized MPs and NPs evidenced by the rapid and excessive production at 24 hours post dosing (Figure 7M and 6O). The acute release of IL-8 at 24 hours was observed in the 30 nm group (Figure 7P). Detectable levels of IL-8 production in 500 nm and 100 nm groups were not observed until 48 hours post exposure (Figure 7O and 7P). In these groups, the mean cytokine levels sustained or kept increasing from 24 to 48 hours but tended to decline after that. Notably, in 1000 μg/mL groups, the TGF-β1 concentrations were significantly elevated by 100 nm particles at 72 hours and by 30nm particles at 48 hours (*p<0.05, Figure 7N). Monolayers were found to be detached from the Transwell inserts in 100 nm groups at 96 hours and 30 nm groups at 72 hours and cytokine data from these groups were not collected.

4. Discussion

Plastics are extensively used in our daily lives and are increasingly contributing to both land and water pollution. Over time, these plastics degrade and generate micro- or nano-sized plastic particles (MPs or NPs). In 2018, microplastics were first reported as present in human feces, providing evidence of accumulation, ingestion, and excretion of these particles in humans and indicating exposure through processed or packaged food/water consumption.[6] Since then, plastics have been detected in human placental tissues[36] and blood[37]. Human exposure to MPs and NPs is growing and the human intestine is the principal exposure site. However, research connecting MPs/NPs with human intestinal cells and tissues is still preliminary. In addition to the MPs and NPs themselves, these particles can release plastic additives and/or adsorb other environmental chemicals, many of which have been shown to exhibit endocrine-disrupting and inflammatory effects.[38] MPs and NPs have also been linked to intestinal diseases. For example, in rodent models and marine organisms, chronic exposure to MPs and NPs has resulted in increased gut permeability, increased expression of pro-inflammatory cytokines and alterations in microbiota composition and function.[8] However, related studies quantifying toxicity or cellular uptake in the human intestine are scarce and lacking in physiologically relevant outcomes. Therefore, there is a need to establish robust human-based in vitro experimental models that can predict in vivo outcomes of MP and NP pollution hazards in the human intestine and also provide a basis for subsequent particle management and control if needed. For these reasons, in the present study, we employed organoid technology to create near physiologically relevant cell culture models for the evaluation of the potential toxic effects of MPs and NPs varying in size (covering micro to nano scales, 1 μm, 500 nm, 100 nm and 30 nm), concentrations (250 μg/mL, 500 μg/mL and 1000 μg/mL), and exposure periods (24, 48, 72 and 96 hours) on patient organoid-derived intestinal epithelia with different cellular complexities (with and without M cells), examining cellular uptake and translocation, and impact on barrier integrity and immune response (cytokine release).

Much of the research concerning in vitro cellular uptake and cytotoxic impact of MPs and NPs in human intestinal epithelium has been carried out using monocultures of Caco2 or HT29-MTX (enterocyte-like or goblet-like cells), co-cultures of Caco-2/HT29-MTX, or tri-cultures of Caco-2/HT29-MTX/Raji B (M-like

cell induction).[18-21, 39] However, these human cancerous cell lines have several limitations. First, these cell cultures have much higher TEER values (1600-2500 $\Omega.cm^2$) than what is reported for the intestine in vivo (50-100 $\Omega.cm^2$), reflecting poorer permeability of compounds through the paracellular route. Second, these cell cultures only represent limited cell subgroups (enterocytes/goblet cells/M-like cells) which do not faithfully mirror the broad diversity of in vivo epithelial cell diversity and therefore fail to reproduce the complexity of in vivo cellular responses. By co-culturing Caco-2 cells with Raji lymphocyte cells, Caco-2 cells can be induced to differentiate into cells with an M-like cell morphology, yet there have been no consistent experimental conditions reported in terms of the onset of the co-culture, the duration of the co-culture, the standardized number of Raji B cells for sufficient M-like cell induction.[40] Third, while representing some subgroups of the intestinal epithelium, these cell lines are cancerous and therefore differ from the normal cells. Systems based on these cancerous cell lines have proved unreliable in terms of reciprocating the biological and physiological function of intestinal epithelial cells due to the low or absent expression of some clinically relevant transporter proteins, including sodium/glucose cotransporter 1(SGLT1) and microsomal triglyceride transfer protein (MTP), and metabolic enzymes, such as cytochrome P450 (CYP) enzymes.[41] It was also reported that Caco-2 cells were particularly resistant to cytotoxic effects of PS NPs.[42] Therefore, nanomaterial toxicity tests using normal and cancer cells may yield significantly different outcomes. As a promising alternative intestinal epithelial model, intestinal organoids can be used to study intestinal nutrient transport along with uptake and metabolism of drugs and exogenous compounds. Through gene expression analysis, researchers have demonstrated that, compared to undifferentiated and differentiated Caco-2 cells, organoid-derived intestinal epithelial cells more appropriately express a panel of metabolically essential genes and some critical genes involved in fatty acid and cholesterol homeostasis in the small intestine.[43] In addition, solute carrier family 5 member 1 (SLC5A1), microsomal triglyceride transfer protein (MTTP), and nuclear receptor subfamily 1 group I member (2NR1I2) genes encoding SGLT1, MTP, and PXR (pregnane X receptor, a CYP expression regulator) are expressed and functional in organoid-derived intestinal epithelial cells.[43] Importantly, intestine organoids also have shown higher toxicity predictability than Caco-2 cells in drug screening study with 31 drugs used clinically as a reference set,[44] suggesting the intestinal organoid models permit more human-relevant prediction of the adverse effects caused by exposures to foreign compounds.

In this context, we adapted human intestinal organoids as a tool to assess MP- and NP-induced toxicity in the human gut. After targeting the cells, different sized particles internalize and pass through the intestinal epithelium by different pathways and mechanisms for them to undergo intracellular transport via regular epithelial cells and M cells, and then exit the cells at the basolateral membrane to complete the absorption process. Accordingly, we generated two physiologically relevant epithelial organoid monolayer models following well-established differentiation protocols (Figure 2): SDM-induced monolayer without M cells (enterocytes, goblet cells, EECs, and Paneth cells) and MDM-induced monolayers with M cells (enterocytes, goblet cells, EECs, and Paneth cells, M cells). Our intention was to simulate in vivo cellular complexity for particle uptake and translocation to identify how different cell models respond to the exposure of MPs and NPs and ultimately decipher the contribution of M cells during these responses. Using immunostaining with various cell specific markers and SEM, we validated that the different protocols successfully induced the undifferentiated monolayers into mature intestinal epithelia with desired cell populations consisting of the major epithelial cell types without/with M cells.

Several studies using in vitro cell models have indicated that the size of particles plays a critical role in determining the efficiency of cellular uptake as well as the uptake pathway in different living human cell. For example, a size-dependent uptake has been observed for PS particles in human lung cells, astrocytoma cells, umbilical vein endothelial cells, intestinal cells (Caco-2).[45] In all cases, smaller particles had a higher chance of penetrating the cell membrane, demonstrating larger adverse effects, and the particles had maximal cellular uptake in the size range of 30-50nm. Therefore, in our study, we examined the size-dependance of the cellular uptake and translocation of MPs and NPs (1μm, 500nm, 100nm and 30nm) in the organoid-derived intestinal epithelia (Figures 3, 4, 5). Our results showed that, in SDM-induced intestinal epithelia, all MPs and NPs homogeneously attached to and potentially entered via the apical side

of the epithelial surface with a significant uptake only occurring at the particle size of 30nm at 96 hours after exposure. In contrast, in the monolayers containing M cells (MDM-induced cell cultures), while the cellular internalization of the MPs and NPs was also highly dependent on the size, plastic particles larger than 500nm preferentially aggregated in M cells and penetrated the monolayers through M cells. In addition, the incorporation of M cells generally increased the degree of translocation of MPs and NPs at all sizes. Particularly, 30nm particles were randomly taken up by regular epithelial cells (enterocytes and secretory cells), whereas larger particles (500nm and 1μm) crossed the epithelium via M cells. This finding is supported by earlier in vivo data demonstrating that larger PS particles are taken up exclusively by M cells associated with Peyer's patch in rats and mice[46] and in vitro data showing M-like cells from cancerous cell lines and M-cells induced from mouse intestinal organoids were strongly associated with higher uptake of PS NPs.[47] A key characteristic of functional M-cells is that they can efficiently capture and transport large particles and bacteria across the epithelial barrier. In this regard, M cells induced from intestinal organoids exhibit similar functional characteristics to M-cells in vivo, confirming the potential of intestinal organoids as a platform for enriching and studying rare intestinal cell types, such as M cells, EECs, Tuft cells.[48] Moreover, our results also agreed with the accepted mechanism of microparticle (i.e. > 100nm) uptake through transcytosis across M-cells located in the Peyer's patches and nanoparticle (i.e. <100nm) uptake through other epithelial cells, such as enterocytes and goblet cells, by endocytosis or paracellular transport through tight junctions (only for particles smaller than 5 nm).[49] These results suggest that the cellular translocation mechanism and efficiency of the PS MPs and NPs in human intestine significantly relies on the particle size.

After observing the differences in internalization behaviors with MPs and NPs in different sizes, we further evaluated two other experimental variables, concentration and exposure period, on the cytotoxic impact of the particles on intestinal epithelial cells by examining the epithelial barrier integrity using TEER and immune response using ELISA-based cytokine measurement (Figures 5, 6). Given that MPs and NPs accumulate in the gut of several living organisms and that large plastic debris may even block the gastrointestinal track in some severe cases,[50] we decided on screening extreme effects of PS particles using high concentrations ranging from 250 to 1000 μg/mL. Many of the available studies have used similar concentration ranges to assess the biological effects of PS MPs and NPs in intestinal or other cell types,[4, 51, 52] with some studies testing even higher particle doses (up to 2000 μg/mL).[53, 54]

For TEER measurement, we observed a significant reduction in TEER values in the epithelia containing M cells (396-495 $\Omega*cm^2$) compared to the epithelia without M cells (627-726 $\Omega*cm^2$) (Figures 2L and 2M). This can be explained by a synergistic effect of: 1) the addition of RANKL and TNF-α, which are not only M-cell inducers but also inflammatory cytokines-cytokines promoted inflammation, leading to a decrease in TEER, and 2) the increased presence of M cells which may have disrupted tight junction formation among enterocytes, increasing the permeability of the overall cell layer. It has been shown previously that M-cell formation in epithelial monolayers led to decreased TEER values.[55] Human intestine maintains a low-grade "physiological inflammation", which is orchestrated by the tissue microenvironment, to combat invading pathogens.[56] Our result may suggest that the addition of the cytokines to the basolateral side of the cells in our system somehow incurs the ideal "physiological inflammation", which also explained why MDM-treated epithelia showed slightly elevated levels of cytokines compared with the SDM-treated epithelia in the control groups (Figures 6 and 7). TEER values reported for GI tract models reveal that the in vivo small intestinal epithelium exhibits TEER values in the rage of 50-100 $\Omega.cm^2$, whereas the large intestine (colon) generates values in the range of 300-400 $\Omega.cm^2$.[35] In this perspective, M cell containing epithelia are more comparable to the in vivo conditions, providing more realistic models for permeability studies.

During the plastic exposure experiments, we did not observe obvious changes in the TEER values in the SDM-induced epithelia exposed to 1 μm, 500 nm, 100 nm particles, independent of the concentrations (250 μg/mL, 500 μg/mL, and 1000 μg/mL), and exposure period (24, 48, 72 and 96 hours). Similar results were obtained in the MDM-induced epithelia treated with 1μm and 500 nm MPs. This is in line with work from

other groups employing either differentiated or undifferentiated Caco-2 cells, in which no or slight impact on cell viability and membrane integrity was found when exposed to PS particles (100 nm-5 μm). It is worth noting that the highest concentration tested in these studies was 200μg/mL and the longest exposure time in the experiments was 48 hours.[57] As an exception, 5 μm PS-MPs inhibited the proliferation of Caco-2 cells in vitro in a time- and concentration-dependent pattern.[58] However, in that study Caco-2 cells were cultured in planar plastic substrate, which could affect the cell growth and differentiation and therefore lead to discrepancies in the results. Our data obtained from human derived intestinal organoids (with and without M cells) supplement the existing knowledge regarding PS particle toxicity by showing even higher concentrations of particles larger than 500 nm (500 nm and 1 μm) with prolonged exposure time (up to 96 hours) did not lead to obvious damage to the intestinal epithelial integrity. Additionally, in the exposure study, as the concentration of particles was increased to 1000 μg/mL, 30 nm NP exposure groups mildly induced decreases in TEER in SDM-induced epithelia, whereas both the 100 nm and 30 nm groups significantly decreased TEER in the MDM-induced monolayer starting from 48 hours of exposure. It is worth mentioning that, compared to the control groups, in the monolayers without M cells, cell viability did not seem to be significantly affected by MPs and NPs. However, intestinal monolayers containing M cells detached in the groups of 100 nm/96hour, 30 nm/72hour and 30 nm/96hour at a concentration of 1000 μg/mL, indicating cell death during exposure to smaller sized groups. This observation agrees with previous reports documenting that smaller sized nanoparticles are correlated with higher cell damage in both in vitro and in vivo models[5] and that additionally, PS particles do not cause notable cytotoxicity in human skin dermal fibroblasts and blood cells at concentrations up to 500 μg/mL.[23] Interestingly, both 30 nm and 100 nm groups resulted in more progressive reduction of TEER in the M cell containing epithelia.

The mechanisms of MPs and NPs cytotoxicity also involve stimulating the secretion of inflammatory cytokines. Cytokines represent a vast family of immunomodulatory substances typically including Interleukins (IL), Interferon (IFN), Growth Factor (GF), Tumor Necrosis Factor (TNF), and Chemokines (CKs).[56] As above-mentioned, maintaining a low-grade "physiological inflammation" in the essential for normal tissue function. During the infection or injury, multiple intestinal immune and non-immune cells release abundant counter-regulatory cytokines to enable gut immune homeostasis and tolerance. Dysfunction of cytokine release by the immune system in host epithelial cells has been implicated in inflammatory bowel disease (IBD), which affects approximately 3.1 million adults (1.3%) in the United States and more than 10 million people worldwide. Among different cytokines, the most studied members involved in intestinal immune inflammation comprise TNF-α, TGF-β1, IL-6 and IL-8. In this study, we quantified the release of TNF-α, TGF-β1, IL-6 and IL-8 in the monolayers to understand whether treatment with PS MPs and NPs triggers an inflammatory response in the intestinal epithelium. We also investigated whether the cytokine secretion occurred in a size-, concentration- or exposure period- dependent manner.

TNF-α is considered a proinflammatory substance produced by bone marrow-derived macrophages and many other cells, such as lymphocytes and mast cells. TNFα was upregulated in intestinal biopsies from active Crohn's disease patients.[59] Transforming growth factor-β (TGF-β) is a highly multifunctional cytokine released by leukocytes, stromal cells, and epithelial cells. TGF-β targets practically all the intestinal mucosal cell types and exerts a wide range of actions regulating the restoration of intestinal epithelial barrier in vivo.[60] IL-6 acts as both pro-inflammatory and anti-inflammatory cytokine and its secretion level is readily and transiently promoted in response to tissue damage and infections to provide host defense and repair by evoking an acute inflammatory response. IL-6 is increased in biopsy specimens from IBD patients.[61] IL-8 is a chemoattractant cytokine known to be produced by a wide array of tissue cells. The expression levels of IL-8 in the human intestine are linked to the immune response in the colon tissue samples of patients with ulcerative colitis.[62]

Because of the lack of standardized research models and high diversity of the MP and NPs (different size, shape, surface charging and polymer type) used in different studies, there are contradictory results derived from both in vivo and in vitro studies on whether MPs and MPs activate inflammatory reactions in the intestine.[63] For example, in mouse models, one study showed that after 21-weeks of exposure to

environmentally relevant doses of large PS MPs (40-100 μm), mice displayed a clear intestinal inflammatory response with infiltration of immune cells.[64] Similarly, intestinal barrier dysfunction and cell death was found in mice that had been administered PS particles in varying sizes (50 nm, 500 nm and 5000 nm) under single or co-exposure conditions in a size-dependent manner.[65] In contrast, 5 μm PS MPs alone caused minimal effects on the intestinal barrier of mice, but exposure to PS MPs resulted in histological injury, intestinal microbiota disorders, inflammation, and oxidative stress in mice with acute and chronic colitis.[66] A more recent study compared the effects of PS MPs (5 μm) on healthy mice and mice with intestinal immune imbalances. The authors concluded that PS MPs exposure only significantly stimulated the expression of inflammation factors (TNFα, IL-1β and IFN-γ) in mice with intestinal immune imbalance.[67] Data from in vitro human intestinal cell models also contributed to the conflicting results. Some studies have cited that 5 μm PS particles showed little influence on IL-8 and MCP-1 secretion in Caco-2 cells, however, IL-8 levels were enhanced by exposure to 100 nm particles at a concentration of 20 μg/mL.[68] Other studies highlighted that 3 and 10 μm gave rise to a large amount of reactive oxygen species (ROS) production, key signaling molecules in inflammatory disorders, in human intestinal cells in the short term.[19] In the current study, from the cytokine profiles, compared to the non-dosing control groups, virtually no cytokine release was induced until concentrations reached 500 μg/mL in both SDM- and MDM induced intestinal epithelia. Additionally, based on the general increase level of the cytokines in 500 μg/mL and 1000 μg/mL groups, the exposure of PS MPs and NPs induced stronger inflammatory reaction on monolayers without M cells than without M cells. For example, we found that under 1000 μg/mL, both 500 nm and 1 μm MPs significantly induced the secretion of TNF-α, IL-6 and IL-8 compared to the control group, which did not occur in the monolayers without M cells. The key role of the M cells is to sense, capture and deliver antigens/pathogens across the epithelium, thus triggering mucosal immune response. In our case, the larger particles (500 nm and 1μm) were sensed, sampled, and transported through M cells (confirmed in our tracking assay) which led to production of pro-inflammatory cytokines for protection against potential antigens and pathogens. Furthermore, TGF-β1, not promoted in monolayers without M cells in exposure group, was significantly upregulated in 100 nm/72hour and 30 nm/48hour exposure groups. As a pleiotropic cytokine, the role of TGF-β1 in IBD is still under debate. However, most researchers believe that TGF-β inhibits the intestinal inflammatory responses to luminal bacteria and food antigens, thus achieving immune tolerance.[69] In this scenario, when exposed to small PS particles, M cells contribute to the activation the specific immunological pathways (TGF-β signaling pathway) to downregulate excessive inflammatory cytokine release and ameliorate epithelial inflammation caused by particle exposure.[70] However, we also found cell death in the in the groups of 100 nm/96hour, 30 nm/72hour and 30 nm/96hour at a concentration of 1000 μg/mL in the monolayers containing M cells, which did not occur in the monolayer without M cells. This may indicate that the anti-inflammatory activity against small particles triggered by M cells and other epithelial cells was not intense enough to suppress the "cytokine storm" resulting from the sudden and acute increase in levels of TNF-α, IL-6 and IL-8 in the groups with cell death (Figures 7M, 7O, and 7P). Other immune sensers, such as B cells in gut-associated lymphoid tissue (GALT), macrophages, dendritic cells, and mast cells should be involved to reach native immune protection.[71] Based on these findings, we concluded that the ingestion of PS MP and NP suggests the potential towards IBD-related risks via the induced inflammatory cytokines associated with IBD. Furthermore, M cells induced from human intestinal organoids were able to imitate the biological functions of native M cells and that the MDM-induced monolayer represents an improved intestinal follicle-associated epithelium to study MPs and NPs transport by M cells.

5. Conclusions

Intestinal organoids are a powerful tool to evaluate the interactions between the intestinal epithelium and PS plastic particles. We compared the uptake, translocation, and potential cytotoxic effects of the particles in organoid derived monolayers both with and without M cells. We showed that human intestinal epithelial cells internalized PS-NPs in a size-, concentration-, and time-dependent manner as assessed by barrier function and intestinal immune responses in two different intestinal organoid-derived epithelial models (with and without M cells). We noted that larger particles (≥ 500 nm) were taken up predominantly by M

cell-mediated transcytosis, although other epithelial crossing routes may be involved. Furthermore, we found that plastic particles larger than 500 nm were not cytotoxic to intestinal epithelial cells under normal conditions but may provoke tissue damage at very extremely high concentrations under long term exposures. Conversely, smaller particles (≤ 100 nm) yielded toxicity and the epithelium containing M cells were more sensitive to cytotoxicity when compared to the epithelium without M cells. Considering the size effects on the uptake and translocation of MPs and NPs and the simultaneous presence of particles with varying sizes in the environment. Further studies on the uptake and impact of mixed plastic particles with different sizes and chemistries need to be conducted. Intestinal monolayers derived from patient organoids mimic the cell complexity and function of the small intestinal epithelium and provide a valuable tool to study these phenomena in vitro.

Acknowledgements

This work was performed in part at the Harvard University Center for Nanoscale Systems (CNS), a member of the National Nanotechnology Coordinated Infrastructure Network (NNCI). Figures 2A and 3A were created with BioRender.com.

Funding Statement

We thank the NIH (U19-AI131126, P41EB027062) and NSF DMR2104294 for support of this work.

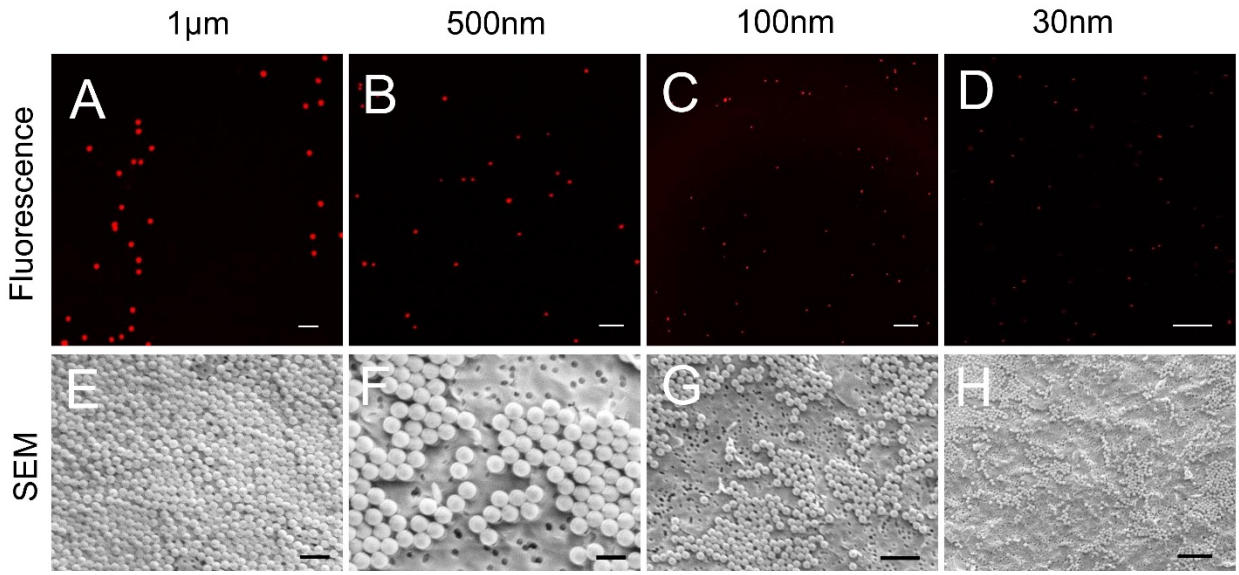

Figure 1. Characterization of polystyrene particles. (A-D) Representative fluorescence microscope images confirmed the fluorescence of MPs and NPs, respectively, (A)1 μm MPs, scale bar: 5 μm, (B) 500 nm, scale bar: 5 μm, (C) 100 nm, scale bar: 1 μm and (D) 30 nm, scale bar: 500 nm. (E-H) SEM images of 1 μm MPs (E, scale bar: 3 μm), 500 nm MPs (F, scale bar: 1 μm), 100 nm (G, scale bar: 500 nm) and 30 nm (H, scale bar: 300 nm).

Table 1. Characterization and validation of the parameters of polystyrene MPs and NPs by SEM image analysis

PS MPs and NPs	N	Mean particle size	Standard deviation	Particle size range
30 nm	25	30.06 nm	±0.63 nm	28.56-31.82 nm
100 nm	50	99.72 nm	±1.61 nm	97.13-104.25 nm
500 nm	25	500.06 nm	±2.65 nm	494.92-503.89 nm
1 μm	100	1.02 μm	±0.08 μm	0.87-1.25 μm

PS MPs and NPs	**N**	**Mean particle size**	**Standard deviation**	**Particle size range**
30nm	25	30.06nm	±0.63nm	28.56-31.82nm
100nm	50	99.72nm	±1.61nm	97.13-104.25nm
500nm	25	500.06nm	±2.65nm	494.92-503.89nm
1μm	100	1.02μm	±0.08μm	0.87-1.25μm

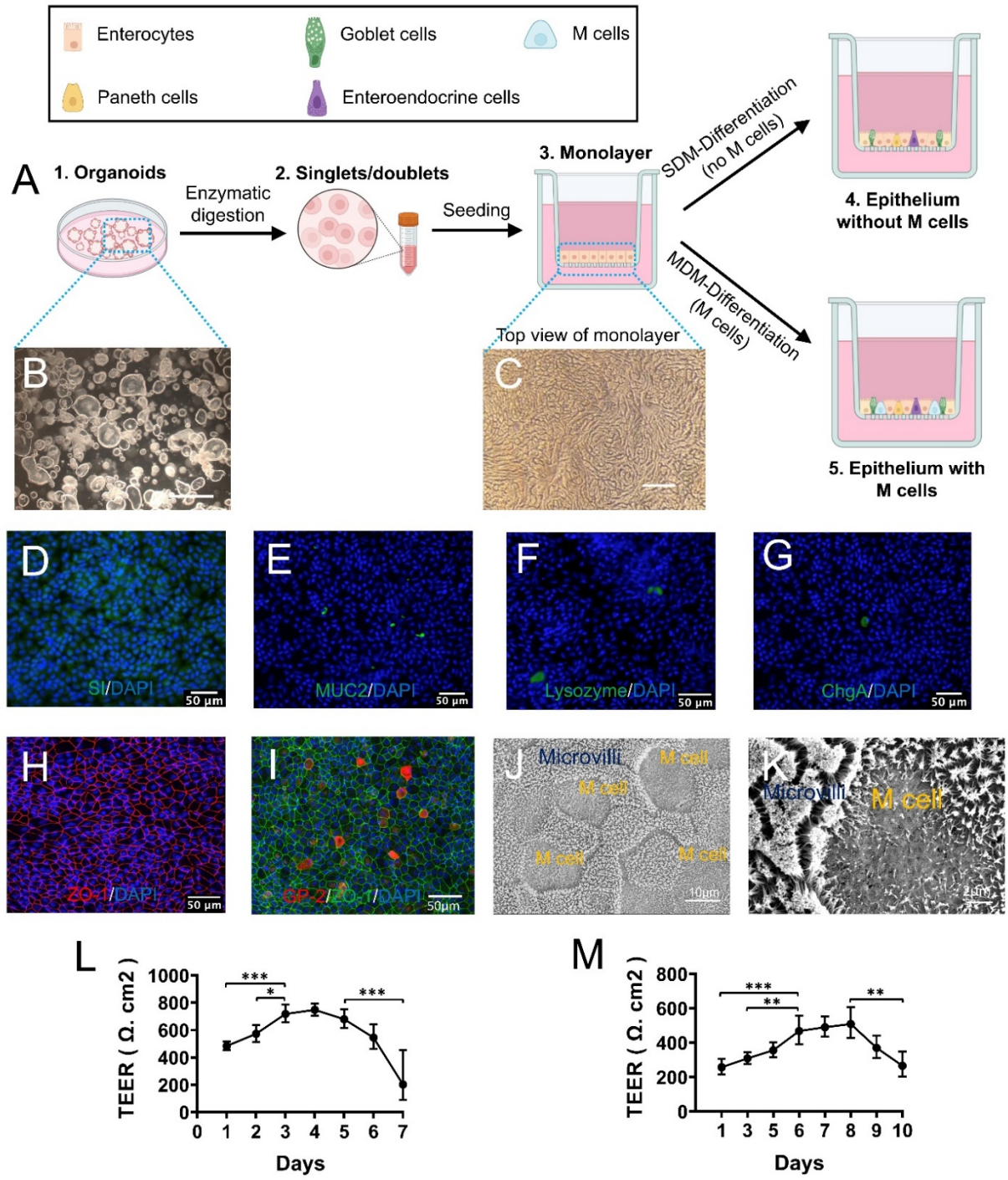

Figure 2. Establishment and characterization of SDM- and MDM differentiated monolayer cell cultures from intestinal organoids. (A-C) Organoid culture and the monolayer formation. Organoid (A1, B) were expanded, enzymatically digested into singlets and doublets (A2) and seeded on transwell inserts to form confluent monolayer (A3, C) for differentiation without M cells (A4) and with M cells (A5). (D-H) Immunofluorescence of intestinal epithelial cell differentiation markers in organoid-derived cells stimulated to differentiate with SDM or MDM: staining of SI (D, green), a marker of enterocytes; expression of MUC2 (E, green) a marker of goblet cells; expression of Lysozyme (F, green), a Paneth cell

marker; staining of ChgA (G, green), an EEC marker; expression of tight junction marker, ZO-1 (H, red), and staining of M cell surface marker GP2 (I, red) with tight junction ZO-1 (I, green). Nuclei are counterstained with DAPI (blue). Scale bars: 50 µm. (J-K) SEM images showed "bald" M cells as labeled and polarized microvilli of epithelial cells. Scale bars: (J) 10 µm, (K) 2 µm. (L-M) TEER measurements on SDM-treated (L) and MDM-treated monolayer cultures derived from patient intestinal organoids. (*p < 0.05, **p < 0.005, ***p<0.001).

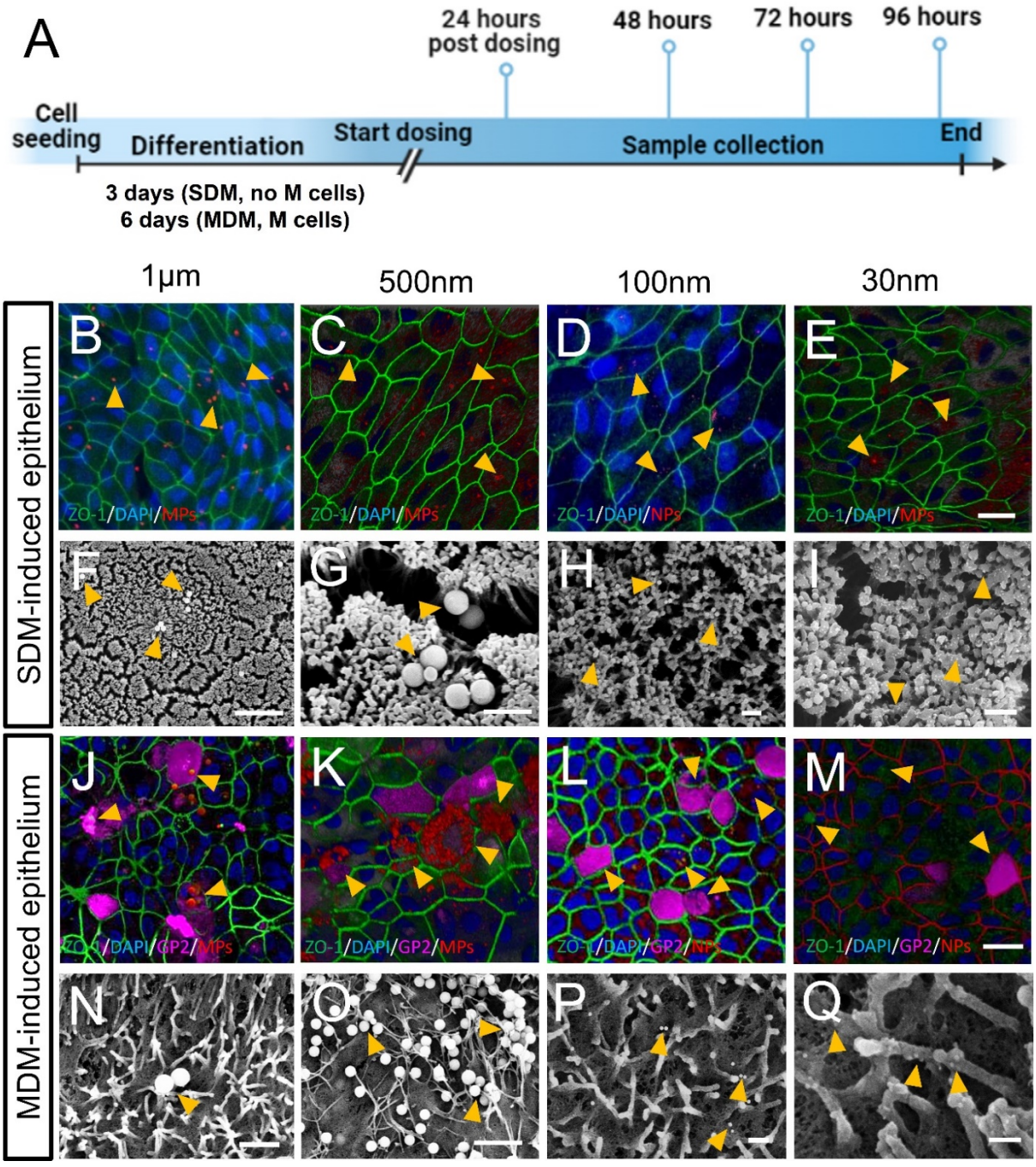

Figure 3. The cellular localization of polystyrene particles. (A) Schematic of the experimental timeline of cell seeding, monolayer differentiation and particle dosing. (B-I) The cellular localization of MPs and NPs

in the SDM-treated epithelium after 24 hours of exposure were visualized by confocal fluorescence microscopy (B-E) and SEM (F-I). (B-E) Representative confocal fluorescence images of SDM-treated monolayers: intestinal epithelium with integral barrier was identified by staining of ZO-1 antibody (green) and particles were seen in red (indicated by yellow arrows). Nuclei were counterstained with DAPI (blue). Scale bars: 10 μm. (F-I) SEM images confirmed the cellular binding of different sized particles to the epithelial microvilli (yellow arrows). Scale bars: (F) 10 μm, (G) 1 μm, (H) 500 nm, (I) 500 nm. (J-Q) The cellular localization of MPs and NPs in the MDM-treated epithelium after 24 hours of exposure were visualized by confocal fluorescence microscopy (J-M) and SEM (N-Q). (J-M) Confocal fluorescence images of MDM-treated monolayers: the fluorescence colors of cells and particles were the same as abovementioned in the SDM-treated cells. M cells were stained with GP2 antibody (magenta). Co-localization of 1 μm and 500 nm with M cells is indicated by yellow arrows. Scale bars: 10 μm. (N-Q) Zoom-in SEM images of M cell surface confirmed the cellular binding and aggregation of different sized particles to the M cell surface with sparse disorganized stubby microvilli (yellow arrows). Scale bars: (N, O) 2 μm, (P) 1 μm, (Q) 500 nm.

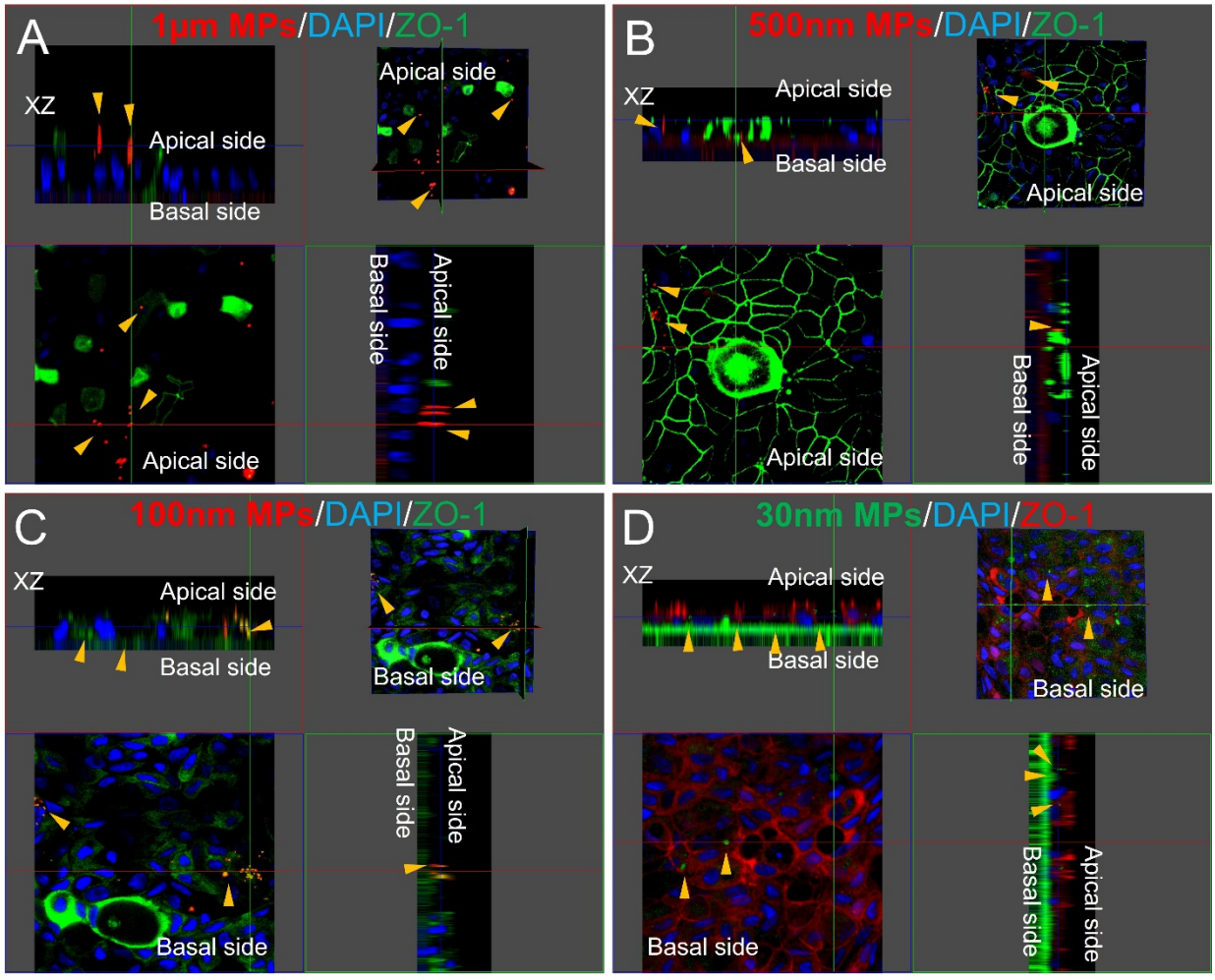

Figure 4. The intracellular translocation of MPs and NPs in the SDM-differentiated culture systems were tracked for up to 96 hours by confocal laser scanning microscopy with 3D z-stack reconstruction. 3D z-

stack reconstruction of the monolayers after exposure to 1 μm MPs (A), 500 nm MPs (B), 100 nm (C) and 30 nm (D) for 96 hours. Intestinal epithelium with integral barrier was identified by staining of ZO-1 antibody (green in A-C, red in D) and 1 μm, 500 nm and 100 nm particles were seen in red, while 30 nm particles were see in green (indicated by yellow arrows). Nuclei were counterstained with DAPI (blue).

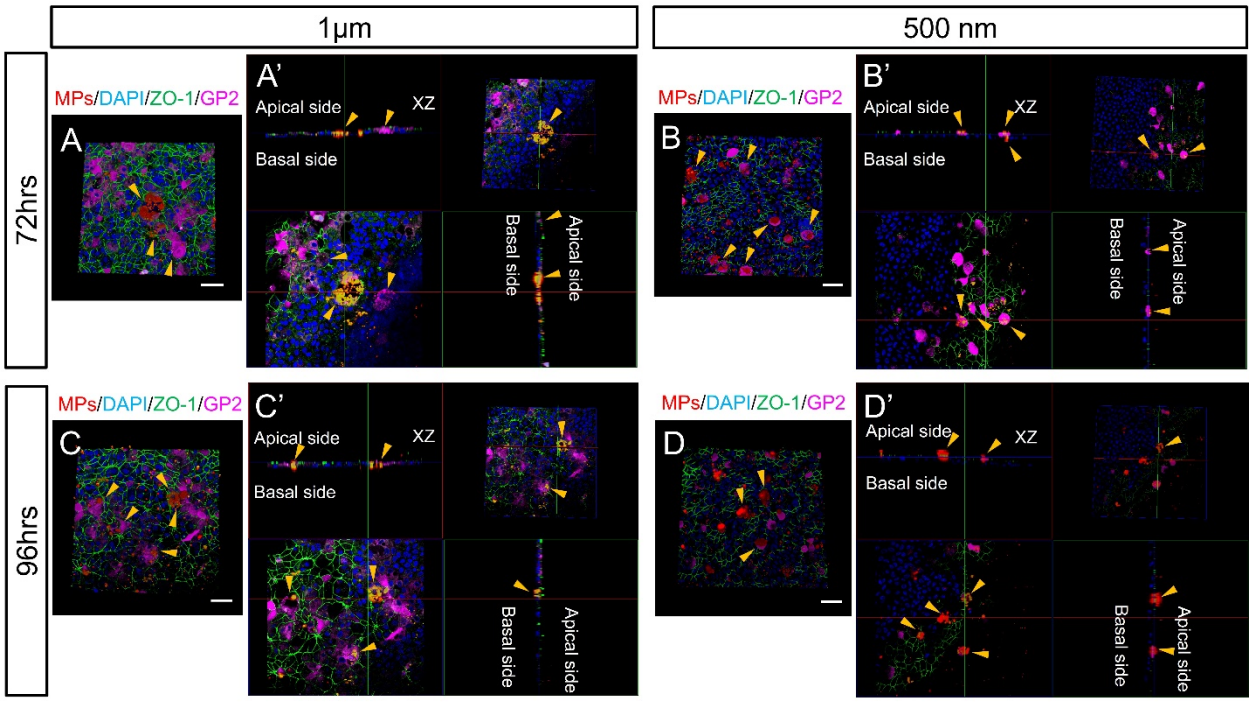

Figure 5. The intracellular translocation of MPs and NPs in the MDM-differentiated culture systems were tracked for up to 96 hours by confocal laser scanning microscopy with 3D z-stack reconstruction. 3D z-stack reconstruction of the monolayers after exposure to 1 μm MPs (A and A') and 500 nm MPs (B and B') for 72 hours and 1 μm MPs (C and C') and 500 nm (D and D') for 96 hours. Intestinal epithelium with integral barrier was identified by staining of ZO-1 antibody (green), M cell was stained by GP2 antibody (magenta), and 1 μm, 500 nm and 100 nm particles were seen in red, indicated by yellow arrows. Scale bars: 20 μm.

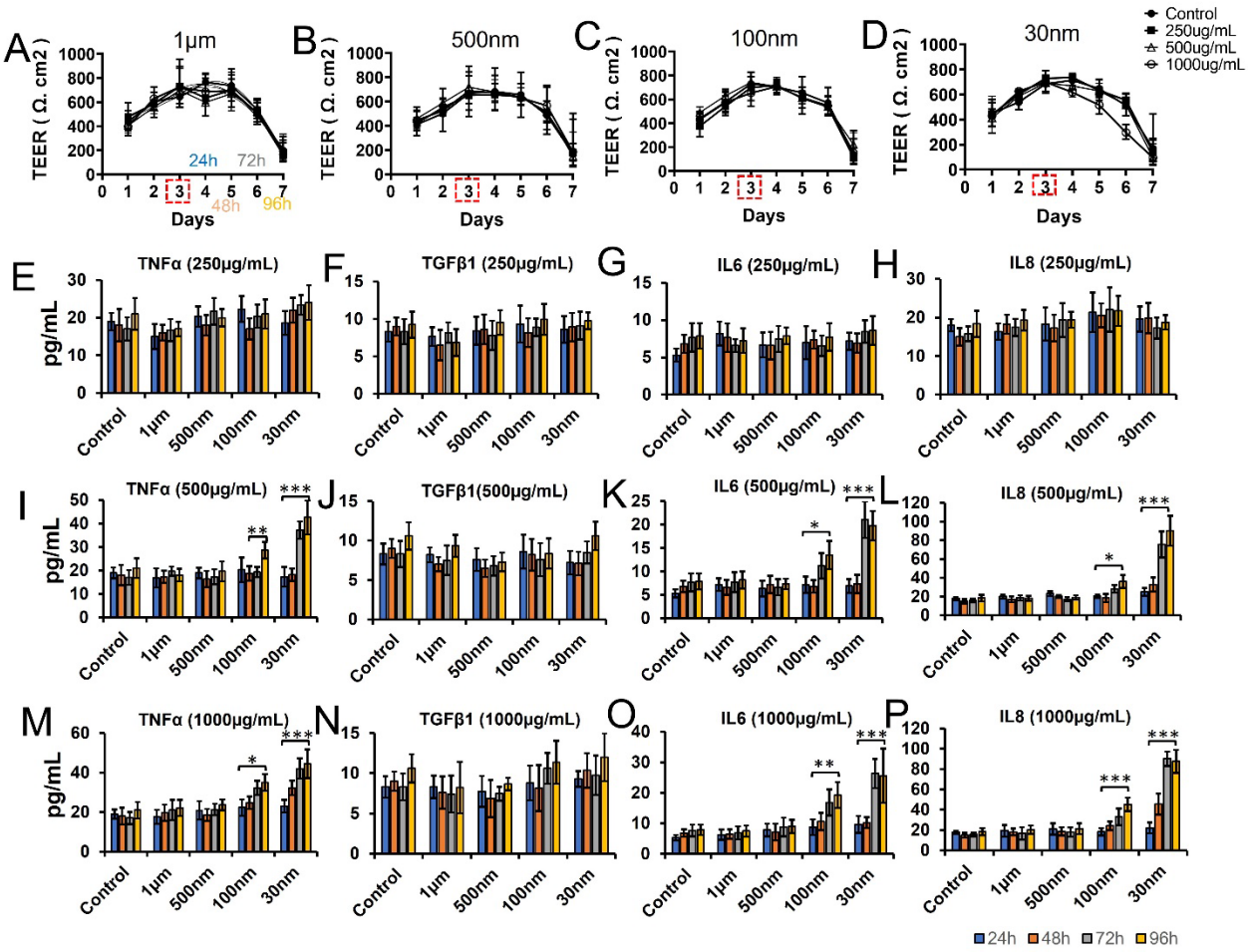

Figure 6. (A-D) TEER measurements of SDM-treated organoid derived epithelial barriers with exposure to 1 μm MPs (A), 500 nm MPs (B), 100 nm NPs (C), and 30 nm NPs (D) at concentrations of 1,000 μg/mL, 500 μg/mL and 250 μL for up to 4 days (96 hours) post expsoure. (E-P) Cytokine profiling of the SDM-treated cultures following exposure to 250 μg/mL, 500 μg/mL and 1000μg/mL were conducted 24, 48, 72 and 96 hours. Inflammatory cytokines including TNF-α (E, I, M), TGF-β1 (F, J, N), IL-6 (G, K, O), and IL-8 (H, L, P) were measured and analyzed. The level of cytokines in the cell supernatant were determined using ELISA. (*$p < 0.05$, **$p < 0.005$, ***$p < 0.001$).

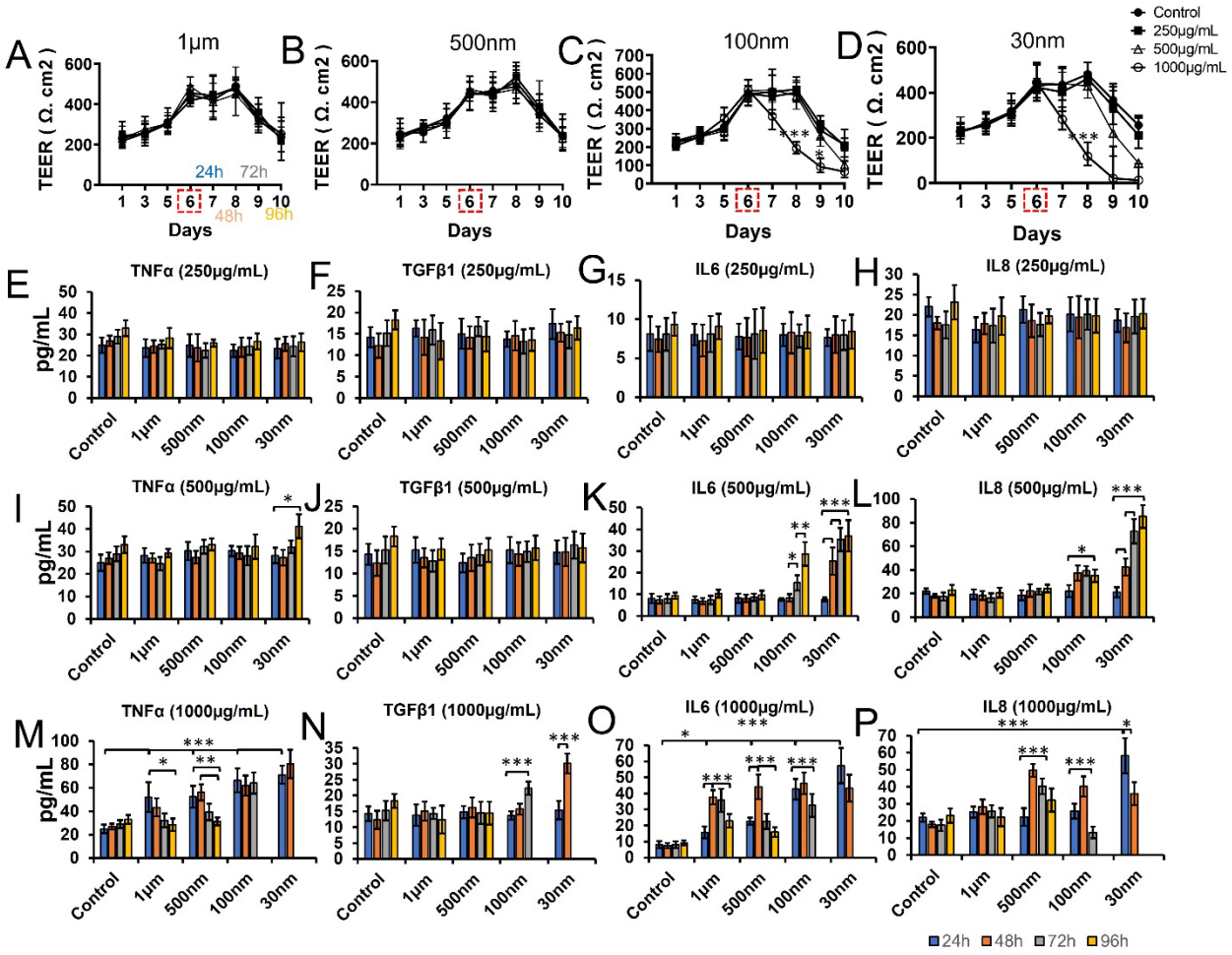

Figure 7. (A-D) TEER measurements of MDM-treated organoid derived epithelial barriers with exposure to 1 µm MPs (A), 500 nm MPs (B), 100nm NPs (C), and 30 nm NPs (D) at concentrations of 1,000 µg/mL, 500 µg/mL and 250 µL for up to 4 days (96 hours) post exposure. (E-P) Cytokine profiling of the MDM-treated cultures following exposure to 250 µg/mL, 500 µg/mL and 1000 µg/mL were conducted 24, 48, 72 and 96 hours. Inflammatory cytokines including TNF-α (E, I, M), TGF-β1 (F, J, N), IL-6 (G, K, O), and IL-8 (H, L, P) were measured and analyzed. The level of cytokines in the cell supernatant were determined using ELISA. (*$p < 0.05$, **$p < 0.005$, ***$p < 0.001$).

6. References

1. Geyer, R., J.R. Jambeck, and K.L. Law, *Production, use, and fate of all plastics ever made.* Science Advances, 2017. **3**(7).
2. Ma, Y., et al., *Effects of nanoplastics and microplastics on toxicity, bioaccumulation, and environmental fate of phenanthrene in fresh water.* Environ Pollut, 2016. **219**: p. 166-173.
3. Ng, E.L., et al., *An overview of microplastic and nanoplastic pollution in agroecosystems.* Sci Total Environ, 2018. **627**: p. 1377-1388.
4. Campanale, C., et al., *A Detailed Review Study on Potential Effects of Microplastics and Additives of Concern on Human Health.* Int J Environ Res Public Health, 2020. **17**(4).
5. Yong, C.Q.Y., S. Valiyaveettil, and B.L. Tang, *Toxicity of Microplastics and Nanoplastics in Mammalian Systems.* Int J Environ Res Public Health, 2020. **17**(5).
6. Schwabl, P., et al., *Detection of Various Microplastics in Human Stool: A Prospective Case Series.* Ann Intern Med, 2019. **171**(7): p. 453-457.
7. Senathirajah, K., et al., *Estimation of the mass of microplastics ingested - A pivotal first step towards human health risk assessment.* J Hazard Mater, 2021. **404**(Pt B): p. 124004.
8. Walker, T.R., et al., *Micro(nano)plastic toxicity and health effects: Special issue guest editorial.* Environ Int, 2022: p. 107626.
9. Deng, Y., et al., *Tissue accumulation of microplastics in mice and biomarker responses suggest widespread health risks of exposure.* Sci Rep, 2017. **7**: p. 46687.
10. Deng, Y.F., et al., *Evidence that microplastics aggravate the toxicity of organophosphorus flame retardants in mice (Mus musculus).* Journal of Hazardous Materials, 2018. **357**: p. 348-354.
11. Jin, Y.X., et al., *Impacts of polystyrene microplastic on the gut barrier, microbiota and metabolism of mice.* Science of the Total Environment, 2019. **649**: p. 308-317.
12. Deng, Y., et al., *Evidence that microplastics aggravate the toxicity of organophosphorus flame retardants in mice (Mus musculus).* J Hazard Mater, 2018. **357**: p. 348-354.
13. Luo, T., et al., *Maternal exposure to different sizes of polystyrene microplastics during gestation causes metabolic disorders in their offspring.* Environ Pollut, 2019. **255**(Pt 1): p. 113122.
14. Stock, V., et al., *Uptake and effects of orally ingested polystyrene microplastic particles in vitro and in vivo.* Arch Toxicol, 2019. **93**(7): p. 1817-1833.
15. Rafiee, M., et al., *Neurobehavioral assessment of rats exposed to pristine polystyrene nanoplastics upon oral exposure.* Chemosphere, 2018. **193**: p. 745-753.
16. Sinagoga, K.L. and J.M. Wells, *Generating human intestinal tissues from pluripotent stem cells to study development and disease.* EMBO J, 2015. **34**(9): p. 1149-63.
17. Chen, Y., et al., *Robust bioengineered 3D functional human intestinal epithelium.* Sci Rep, 2015. **5**: p. 13708.
18. Gautam, R., et al., *Evaluation of potential toxicity of polyethylene microplastics on human derived cell lines.* Sci Total Environ, 2022. **838**(Pt 2): p. 156089.
19. Visalli, G., et al., *Acute and Sub-Chronic Effects of Microplastics (3 and 10 microm) on the Human Intestinal Cells HT-29.* Int J Environ Res Public Health, 2021. **18**(11).
20. Fournier, E., et al., *Microplastics in the human digestive environment: A focus on the potential and challenges facing in vitro gut model development.* J Hazard Mater, 2021. **415**: p. 125632.
21. Banerjee, A. and W.L. Shelver, *Micro- and nanoplastic induced cellular toxicity in mammals: A review.* Sci Total Environ, 2021. **755**(Pt 2): p. 142518.
22. Forte, M., et al., *Polystyrene nanoparticles internalization in human gastric adenocarcinoma cells.* Toxicol In Vitro, 2016. **31**: p. 126-36.
23. Hwang, J., et al., *Potential toxicity of polystyrene microplastic particles.* Sci Rep, 2020. **10**(1): p. 7391.

24. *Animal Models & Translational Medicine: Quality and Reproducibility of Experimental Design | AISAL Symposium.* Comp Med, 2018. **68**(1): p. 84-94.
25. Kim, J., B.K. Koo, and J.A. Knoblich, *Human organoids: model systems for human biology and medicine.* Nat Rev Mol Cell Biol, 2020. **21**(10): p. 571-584.
26. Almeqdadi, M., et al., *Gut organoids: mini-tissues in culture to study intestinal physiology and disease.* Am J Physiol Cell Physiol, 2019. **317**(3): p. C405-C419.
27. Sato, T. and H. Clevers, *Growing self-organizing mini-guts from a single intestinal stem cell: mechanism and applications.* Science, 2013. **340**(6137): p. 1190-4.
28. Chen, Y., et al., *Bioengineered 3D Tissue Model of Intestine Epithelium with Oxygen Gradients to Sustain Human Gut Microbiome.* Adv Healthc Mater, 2022: p. e2200447.
29. Saxena, K., et al., *Human Intestinal Enteroids: a New Model To Study Human Rotavirus Infection, Host Restriction, and Pathophysiology.* J Virol, 2016. **90**(1): p. 43-56.
30. Fasciano, A.C., et al., *Induced Differentiation of M Cell-like Cells in Human Stem Cell-derived Ileal Enteroid Monolayers.* J Vis Exp, 2019(149).
31. Matsui, T. and T. Shinozawa, *Human Organoids for Predictive Toxicology Research and Drug Development.* Front Genet, 2021. **12**: p. 767621.
32. Chen, Y., et al., *In vitro enteroid-derived three-dimensional tissue model of human small intestinal epithelium with innate immune responses.* PLoS One, 2017. **12**(11): p. e0187880.
33. Roh, T.T., et al., *3D bioengineered tissue model of the large intestine to study inflammatory bowel disease.* Biomaterials, 2019. **225**: p. 119517.
34. Chen, Y., et al., *Bioengineered 3D Tissue Model of Intestine Epithelium with Oxygen Gradients to Sustain Human Gut Microbiome.* Adv Healthc Mater, 2022. **11**(16): p. e2200447.
35. Srinivasan, B., et al., *TEER measurement techniques for in vitro barrier model systems.* J Lab Autom, 2015. **20**(2): p. 107-26.
36. Ragusa, A., et al., *Plasticenta: First evidence of microplastics in human placenta.* Environ Int, 2021. **146**: p. 106274.
37. Leslie, H.A., et al., *Discovery and quantification of plastic particle pollution in human blood.* Environ Int, 2022. **163**: p. 107199.
38. Yin, C., et al., *Changes of the acute and chronic toxicity of three antimicrobial agents to Daphnia magna in the presence/absence of micro-polystyrene.* Environ Pollut, 2020. **263**(Pt A): p. 114551.
39. Wang, Q., et al., *Effects of bisphenol A and nanoscale and microscale polystyrene plastic exposure on particle uptake and toxicity in human Caco-2 cells.* Chemosphere, 2020. **254**: p. 126788.
40. Dillon, A. and D.D. Lo, *M Cells: Intelligent Engineering of Mucosal Immune Surveillance.* Front Immunol, 2019. **10**: p. 1499.
41. Vaessen, S.F., et al., *Regional Expression Levels of Drug Transporters and Metabolizing Enzymes along the Pig and Human Intestinal Tract and Comparison with Caco-2 Cells.* Drug Metab Dispos, 2017. **45**(4): p. 353-360.
42. Domenech, J., et al., *Long-Term Effects of Polystyrene Nanoplastics in Human Intestinal Caco-2 Cells.* Biomolecules, 2021. **11**(10).
43. Takahashi, Y., et al., *Organoid-derived intestinal epithelial cells are a suitable model for preclinical toxicology and pharmacokinetic studies.* iScience, 2022. **25**(7): p. 104542.
44. Peters, M.F., et al., *Human 3D Gastrointestinal Microtissue Barrier Function As a Predictor of Drug-Induced Diarrhea.* Toxicol Sci, 2019. **168**(1): p. 3-17.
45. Paul, M.B., et al., *Micro- and nanoplastics - current state of knowledge with the focus on oral uptake and toxicity.* Nanoscale Adv, 2020. **2**(10): p. 4350-4367.
46. Jung, C., J.P. Hugot, and F. Barreau, *Peyer's Patches: The Immune Sensors of the Intestine.* Int J Inflam, 2010. **2010**: p. 823710.

47. Tong, T., et al., *Transport of artificial virus-like nanocarriers through intestinal monolayers via microfold cells.* Nanoscale, 2020. **12**(30): p. 16339-16347.
48. Boonekamp, K.E., T.L. Dayton, and H. Clevers, *Intestinal organoids as tools for enriching and studying specific and rare cell types: advances and future directions.* J Mol Cell Biol, 2020. **12**(8): p. 562-568.
49. da Silva, A.B., et al., *Gastrointestinal Absorption and Toxicity of Nanoparticles and Microparticles: Myth, Reality and Pitfalls explored through Titanium Dioxide.* Curr Opin Toxicol, 2020. **19**: p. 112-120.
50. Lear, G., et al., *Plastics and the microbiome: impacts and solutions.* Environ Microbiome, 2021. **16**(1): p. 2.
51. Chen, Y.C., et al., *The nephrotoxic potential of polystyrene microplastics at realistic environmental concentrations.* J Hazard Mater, 2022. **427**: p. 127871.
52. Rudolph, J., et al., *Noxic effects of polystyrene microparticles on murine macrophages and epithelial cells.* Sci Rep, 2021. **11**(1): p. 15702.
53. Sarma, D.K., et al., *The Biological Effects of Polystyrene Nanoplastics on Human Peripheral Blood Lymphocytes.* Nanomaterials (Basel), 2022. **12**(10).
54. Zhang, Y.X., et al., *Bioaccumulation of differently-sized polystyrene nanoplastics by human lung and intestine cells.* J Hazard Mater, 2022. **439**: p. 129585.
55. Ude, V.C., et al., *Using 3D gastrointestinal tract in vitro models with microfold cells and mucus secreting ability to assess the hazard of copper oxide nanomaterials.* J Nanobiotechnology, 2019. **17**(1): p. 70.
56. Kany, S., J.T. Vollrath, and B. Relja, *Cytokines in Inflammatory Disease.* Int J Mol Sci, 2019. **20**(23).
57. Domenech, J., et al., *Interactions of polystyrene nanoplastics with in vitro models of the human intestinal barrier.* Arch Toxicol, 2020. **94**(9): p. 2997-3012.
58. Wu, S., et al., *Effects of polystyrene microbeads on cytotoxicity and transcriptomic profiles in human Caco-2 cells.* Environ Toxicol, 2020. **35**(4): p. 495-506.
59. Vavricka, S.R., et al., *Expression Patterns of TNFalpha, MAdCAM1, and STAT3 in Intestinal and Skin Manifestations of Inflammatory Bowel Disease.* J Crohns Colitis, 2018. **12**(3): p. 347-354.
60. Stolfi, C., et al., *Role of TGF-Beta and Smad7 in Gut Inflammation, Fibrosis and Cancer.* Biomolecules, 2020. **11**(1).
61. Leon, A.J., et al., *High levels of proinflammatory cytokines, but not markers of tissue injury, in unaffected intestinal areas from patients with IBD.* Mediators Inflamm, 2009. **2009**: p. 580450.
62. Okada, T., et al., *IL-8 and LYPD8 expression levels are associated with the inflammatory response in the colon of patients with ulcerative colitis.* Biomed Rep, 2020. **12**(4): p. 193-198.
63. Jin, Y., et al., *Impacts of polystyrene microplastic on the gut barrier, microbiota and metabolism of mice.* Sci Total Environ, 2019. **649**: p. 308-317.
64. Deng, Y., et al., *Long-Term Exposure to Environmentally Relevant Doses of Large Polystyrene Microplastics Disturbs Lipid Homeostasis via Bowel Function Interference.* Environ Sci Technol, 2022. **56**(22): p. 15805-15817.
65. Liang, B., et al., *Underestimated health risks: polystyrene micro- and nanoplastics jointly induce intestinal barrier dysfunction by ROS-mediated epithelial cell apoptosis.* Particle and Fibre Toxicology, 2021. **18**(1): p. 20.
66. Luo, T., et al., *Polystyrene microplastics exacerbate experimental colitis in mice tightly associated with the occurrence of hepatic inflammation.* Sci Total Environ, 2022. **844**: p. 156884.
67. Liu, S., et al., *Polystyrene microplastics aggravate inflammatory damage in mice with intestinal immune imbalance.* Sci Total Environ, 2022. **833**: p. 155198.
68. Liu, S., et al., *Influence of the digestive process on intestinal toxicity of polystyrene microplastics as determined by in vitro Caco-2 models.* Chemosphere, 2020. **256**: p. 127204.

69. Marafini, I., et al., *TGF-Beta signaling manipulation as potential therapy for IBD.* Curr Drug Targets, 2013. **14**(12): p. 1400-4.
70. Kotlarz, D., et al., *Human TGF-beta1 deficiency causes severe inflammatory bowel disease and encephalopathy.* Nat Genet, 2018. **50**(3): p. 344-348.
71. Kurashima, Y., et al., *Extracellular ATP mediates mast cell-dependent intestinal inflammation through P2X7 purinoceptors.* Nat Commun, 2012. **3**: p. 1034.